Title

Three-dimensional assessment of curvature, torsion, and canal flare index of the humerus of skeletally mature nonchondrodystrophic dogs.

Journal

American Journal of Veterinary Research, 78(10)

ISSN

0002-9645

Authors

Smith, Emily J
Marcellin-Little, Denis J
Harrysson, Ola LA
et al.

Publication Date

2017-10-01

DOI

10.2460/ajvr.78.10.1140

Peer reviewed

Three-dimensional assessment of curvature, torsion, and canal flare index of the humerus of skeletally mature nonchondrodystrophic dogs

Emily J. Smith MS
Denis J. Marcellin-Little DEDV
Ola L. A. Harrysson PhD
Emily H. Griffith PhD

Received November 22, 2016.
Accepted January 26, 2017.

From the Department of Biomedical Engineering (Smith) and the Edward P. Fitts Department of Industrial and Systems Engineering (Harrysson), College of Engineering, and the Department of Statistics, College of Sciences (Griffith), North Carolina State University, Raleigh, NC 27695; and the Department of Clinical Sciences, College of Veterinary Medicine, North Carolina State University, Raleigh, NC 27607 (Marcellin-Little). Ms. Smith's present address is Carl Vinson VA Medical Center, 1826 Veterans Blvd, Dublin, GA 31021. Dr. Marcellin-Little's present address is Department of Surgical and Radiological Sciences, School of Veterinary Medicine, University of California-Davis, Davis, CA 95616.

Address correspondence to Dr. Marcellin-Little (djmarcel@ucdavis.edu).

OBJECTIVE
To assess 3-D geometry of the humerus of dogs and determine whether the craniocaudal canal flare index (CFI) is associated with specific geometric features.

SAMPLE
CT images (n = 40) and radiographs (38) for 2 groups of skeletally mature nonchondrodystrophic dogs.

PROCEDURES
General dimensions (length, CFI, cortical thickness, and humeral head offset), curvature (shaft, humeral head, and glenoid cavity), version (humeral head and greater tubercle), and torsion were evaluated on CT images. Dogs were allocated into 3 groups on the basis of the craniocaudal CFI, and results were compared among these 3 groups. The CT measurements were compared with radiographic measurements obtained for another group of dogs.

RESULTS
Mean ± SD humeral head version was –75.9 ± 9.6° (range, –100.7° to –59.4°). Mean mechanical lateral distal humeral angle, mechanical caudal proximal humeral angle, and mechanical cranial distal humeral angle were 89.5 ± 3.5°, 50.2 ± 4.5°, and 72.9 ± 7.8°, respectively, and did not differ from corresponding radiographic measurements. Mean humeral curvature was 20.4 ± 4.4° (range, 9.6° to 30.5°). Mean craniocaudal CFI was 1.74 ± 0.18 (range, 1.37 to 2.10). Dogs with a high craniocaudal CFI had thicker cranial and medial cortices than dogs with a low craniocaudal CFI. Increased body weight was associated with a lower craniocaudal CFI. Radiographic and CT measurements of craniocaudal CFI and curvature differed significantly.

CONCLUSIONS AND CLINICAL RELEVANCE
CT-based 3-D reconstructions allowed the assessment of shaft angulation, torsion, and CFI. Radiographic and CT measurements of shaft curvature and CFI may differ. (*Am J Vet Res* 2017;78:1140–1149)

The 3-D models created with CT images or 3-D modeling technology (eg, a 3-D coordinate measuring machine or 3-D laser scanner) have been used to analyze the morphology of human bones (including the humerus) to help clinicians and researchers better understand the geometry of these bones and assist in the design of orthopedic implants, particularly implants intended for total joint replacement.[1–8] Geometric studies[1,2,7] of the human humerus have involved measuring the radius of curvature of the humeral head; inclination, version, and offset of the humeral head; inclination and version of the greater tubercle; humeral length; angles between several humeral axes; ellipsoid shape of the humeral canal; flexion-extension axis; and width and height of the capitulum.

ABBREVIATIONS

CFI	Canal flare index
mCaPHA	Mechanical caudal proximal humeral angle
mCrDHA	Mechanical cranial distal humeral angle
mLDHA	Mechanical lateral distal humeral angle

The humerus of nonhuman mammals has been evaluated by use of 3-D methods in 2 studies.[8,9] In 1 study[9] involving 89 dogs, shoulder joint lesions and mineralization identified on CT images were compared to clinical findings to investigate causes of thoracic limb lameness. In the other study,[8] the bovine humerus was analyzed by use of finite-element analysis to investigate orientation of the humerus during jumps and falls and to provide information on biomechanics of the humerus. To our knowledge, the 3-D geometry of the canine humerus has not been reported.

Several orthopedic problems, including osteochondritis dissecans and physeal fractures of the proximal physis of the humerus, lead to loss of articular cartilage or abnormal development of the humeral head with secondary osteoarthritis.[9–11] When medical treatment is unsuccessful, surgical options

are limited to arthrodesis or amputation.[10,12] Total shoulder joint replacement could provide an alternative to arthrodesis or amputation. Development of a stem for total shoulder joint arthroplasty in dogs requires better information about the range of humeral geometries. Parameters relevant to the design of a stem include humeral canal dimensions and CFI (ie, ratio of humeral medullary canal sizes in the proximal metaphysis and the diaphysis), shaft curvature, and humeral head dimensions, shape, and offset relative to the long axis of the humerus.

Geometry of the canine humerus has been determined radiographically.[13,14] Humeral angulation was reported in both of these studies, but information on canal curvature and flare was only included in 1 report[14] and was suboptimal for the design of a humeral prosthetic stem because radiographs are vulnerable to artifacts caused by magnification and limb rotation. Also, the accuracy of radiographic measurements of humeral curvature and CFI is not known. Canal flare index of the canine femur has been assessed as part of studies relating to cementless total hip joint replacement. In 1 study,[15] dogs were assigned into 3 groups on the basis of the CFI (stovepipe femurs had a CFI ≤ 1.8, normally shaped femurs had a CFI ranging from 1.8 to 2.5, and champagne-fluted femurs had a CFI ≥ 2.5).

The purpose of the study reported here was to investigate the association between a low and high humeral CFI with specific humeral geometric features, evaluate uniformity of the curvature of the proximal portion of the humerus assessed in 3-D renderings, and assess similarities between the geometry of the humerus in 3-D renderings and the geometry of the humerus in radiographs. We also intended to evaluate whether retrievers and German Shepherd Dogs have a high or low CFI. We hypothesized that high CFI is associated with specific geometric features (eg, having increased shaft curvature or having thicker cortical bone), humeral shaft curvature is uniform, and measurements obtained from 3-D models and radiographs do not differ.

Materials and Methods

Sample

Canine CT reconstructed images for the North Carolina State University Veterinary Hospital between May 2004 and September 2015 were searched to find eligible patients. Inclusion criteria were a CT image with a complete humerus; a mature nonchondrodystrophic skeleton; body weight ≥ 20 kg; no evidence of a humeral fracture, neoplasia, or humeral deformity; and a CT image of sufficient quality to allow reconstruction into a 3-D model. The CT images were considered unacceptable when the thickness or orientation of the image caused the curvature of the humeral head or condyle to be cut off or flattened to an extent whereby accurate measurements could not be obtained. When both humeri of a dog were available for inclusion in the study, a random number generator[a] was used to select a single humerus (left or right) for inclusion.

A total of 788 CT examinations were identified; 92 patients were eligible for inclusion. An a priori power analysis[b] was performed by use of data from a radiographic study[14,15] that involved 62 dogs to determine the number of subjects needed to detect a difference in craniocaudal humeral CFI > 10% between dog groups that had a low and high CFI. The analysis indicated a sample size of 40 (power, 0.91).

Procedures

Patient number, age, sex, breed, and body weight were recorded for all study subjects. The DICOM files were uploaded into commercially available image-processing software,[c] and 3-D models of humeri were created. The humerus, proximal portions of the ulna and radius, and distal portion of the scapula were separated from the rest of the model. The humerus was separated from adjacent bones and was aligned by reslicing the reconstructed images along the line connecting the center of the proximal portion of the shaft at 20% of humeral length to the midpoint of the line joining the humeral epicondyles (anatomic axis). By use of Boolean operations, the portion of the scapula available on the 3-D model was separated from the humerus. Best-fit medullary canal ellipses were created at 20%, 30%, 40%, and 50% of humeral length **(Figure 1)**. Humeral length and cortical thickness along the major and minor axes of the ellipses were measured at 20%, 30%, 40%, and 50% of humeral length. A best-fit cylinder was fitted to the condyle. Datum points were placed at the cranioproximal aspect of the greater tubercle, caudodistal aspect of the medial condyle, center of the medial edge of the best-fit cylinder fitted to the condyle, most distal aspect of the condyle, caudodistal aspect of the humeral head, center of the concavity of the distal aspect of the condyle, and center of the ellipses at 20%, 30%, 40%, and 50% of humeral length. For torsion measurements, best-fit ellipses were created at 8%, 20% (by use of the ellipse drawn to measure cortical thickness), and 75% of humeral length, and a line was drawn along the major axis of these ellipses **(Figure 2)**. At 92% of humeral length, a line was drawn across the caudal aspect of the condyle, as described elsewhere.[16] Humeri were allocated into 3 evenly sized groups on the basis of the craniocaudal CFI: high (CFI > 1.83), medium (1.64 ≤ CFI ≤ 1.83), and low (CFI < 1.64). The number of retrievers and German Shepherd Dogs in each craniocaudal CFI group was recorded.

The 3-D models were transferred to an additive manufacturing modeling software program.[d] Best-fit analytic spheres were fitted to the humeral head and glenoid cavity by use of the triangle wave brush tool. Humeral head and glenoid cavity radii of curvature were recorded. Datum lines were drawn by connecting the center of the sphere fitted to the humeral head and center of the cylinder fitted to the humeral condyle (to determine the mediolateral mechanical axis; Figure 1); center of the sphere fitted to the humeral head and center of the concavity at the distal

aspect of the humerus (to determine the craniocaudal mechanical axis); most cranioproximal aspect of the greater tubercle and caudodistal aspect of the humeral head (to measure the mCaPHA); most cranioproximal aspect of the greater tubercle to center of the shaft at 20% of humeral length (to measure tubercle inclination); center of the sphere fitted to the humeral head and center of the proximal portion of the shaft at 20% of humeral length (to measure humeral head inclination); centers of the ellipses at 20%, 30%, and 40% of humeral length (to measure metaphyseal curvature); center of the ellipses at 30%, 40%, and 50% of humeral length (to measure diaphyseal curvature at the proximal portion of the humerus); most caudodistal aspect of the medial condyle to center of the lateral edge of the cylinder fitted to the humeral condyle (to measure the mCrDHA); and most distal points on the medial and lateral aspects of the humeral condyle (to calculate mLDHA). Datum planes were created to measure humeral head and greater tubercle version, which included a plane containing the medial and lateral epicondyle datum points and anatomic axis, a plane containing the anatomic axis and center of the humeral head sphere datum point, and a plane containing the anatomic axis and most proximal point on the greater tubercle datum point. To measure version, the humerus was viewed from its proximal aspect along the anatomic axis (Figure 2). The plane containing the medial and lateral epicondyles was the baseline plane, with the medial epicondyle as the 0° reference and lateral epicondyle as the ± 180° reference. By use of the planes created, head version was the angle formed by the humeral head and epicondyle planes, and tubercle version was the angle formed by the greater tubercle and epicondyle planes (planes were viewed as lines to determine version). Landmarks cranial to the epicondyle plane had positive values for version, and landmarks caudal to the epicondyle plane had negative values. Humeral head offset (distance from center of the sphere fitted to the humeral head to the anatomic axis), inclination (2-D angle formed by the anatomic axis and the line joining the center of the sphere fitted to the humeral head and a point at 20% of humeral length on the anatomic axis), version (2-D angle from the medial aspect of the shaft), greater tubercle offset (distance from the most proximal aspect of the tubercle to the anatomic axis), inclination (2-D angle formed by the anatomic axis and the line joining the most proximal aspect of the tubercle and a point at 20% of humeral length on the anatomic axis), version (2-D angle from the lateral aspect of the shaft), mLDHA (2-D angle), mCaPHA (2-D angle), mCrDHA (2-D angle),[13] torsion of the proximal portion of the humerus (2-D angle between ellipse axes at 8% and 20% of humeral length), diaphyseal torsion (2-D angle between ellipse axes at 20% and 75% of humeral length), and torsion of the distal portion of the humerus (2-D angle between the ellipse axis at 75% of humeral length and the condyle line at 92% of humeral length) were measured by use of the additive manufacturing modeling software program.

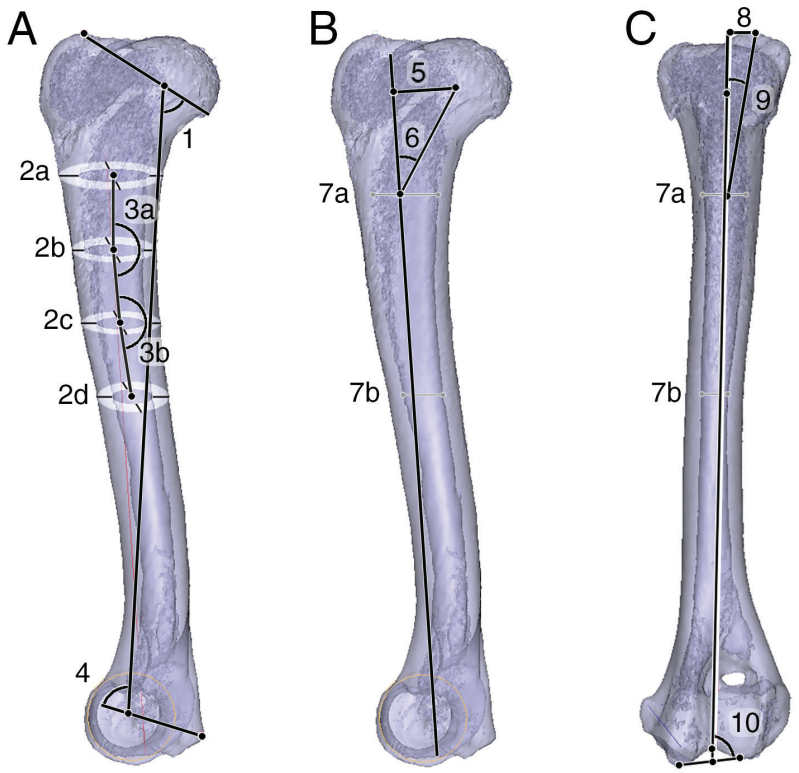

Figure 1—Medial (A and B) and caudal (C) views of drawings of a canine humerus indicating 3-D measurements that were obtained. Measurements included the mCaPHA (1); cortical thickness on the cranial, lateral, caudal, and medial cortices at 20% (2a), 30% (2b), 40% (2c), and 50% (2d) of humeral length; curvature from 20% to 30% of humeral length to 30% to 40% of humeral length (3a), from 30% to 40% of humeral length to 40% to 50% of humeral length (3b), and from 20% to 30% of humeral length to 40% to 50% of humeral length (sum of the 2 previous curvatures); mCrDHA (4); humeral head offset (5); humeral head version (not shown); humeral head inclination angle to 20% of humeral length (6); craniocaudal and mediolateral CFI (ratio of endosteal width at 20% of humeral length [7a] to endosteal width at 50% of humeral length [7b]); greater tubercle offset (8; measured in relation to the anatomic axis [white line]); greater tubercle version (not shown); greater tubercle angle to 20% of humeral length (9; measured in relation to the anatomic axis); and mLDHA (10; measured in relation to the mechanical axis [black line]).

Data analysis

Measurements for a subset of dogs (n = 38) from a previous radiographic study[14] that were nonchondrodystrophic and weighed > 20 kg were obtained and used to compare mechanical and humeral shaft curvature angles. Humeral shaft curvature was measured from 20% to 40%, 30% to 50%, and 20% to 50% of humeral length. Mean ± SD values for mLD-

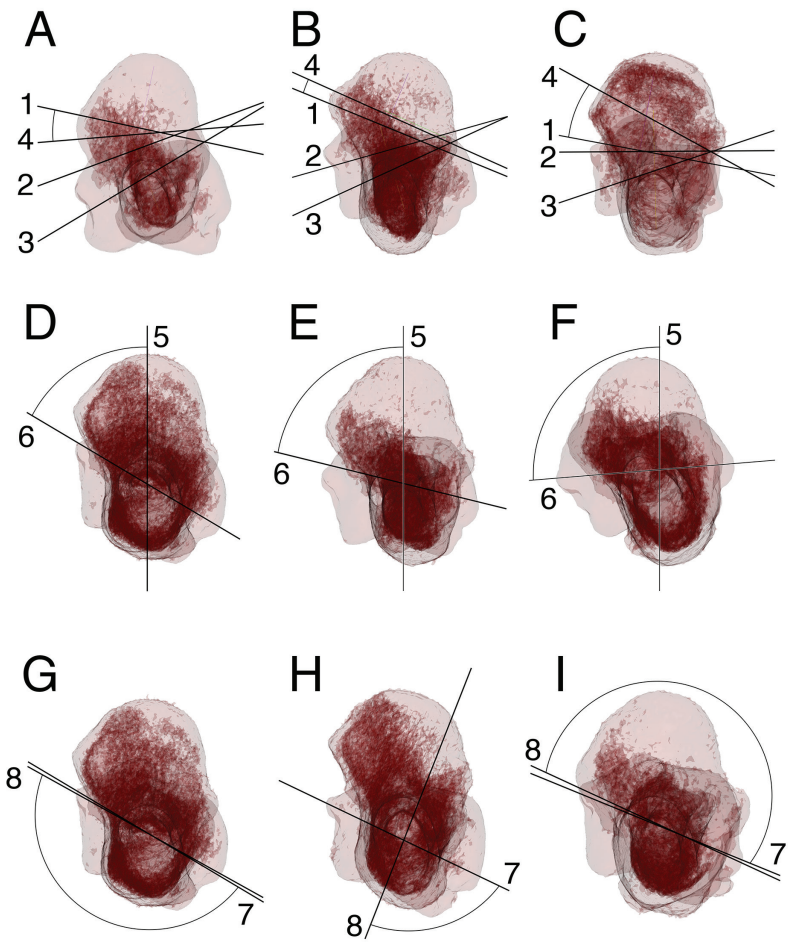

Figure 2—Three-dimensional drawings of the distal aspect of a canine humerus that provide a range for torsion of the humeral shaft (A through C), version of the humeral head (D through F), and version of the greater tubercle (G through I). Each bone is oriented so that the anatomic axis is viewed as a point, the humeral head center (datum) plane is viewed as a vertical line, and the lateral aspect is on the left. For panels A through C, torsion for the proximal portion of the humeral shaft is the angle between lines drawn across the minor axes of ellipses at 8% (line 1) and 20% (line 2) of humeral length; torsion for the diaphyseal portion of the humeral shaft is the angle between line 2 and a line drawn at 75% of humeral length (line 3), and torsion for the distal portion of the humerus is the angle between line 3 and a line drawn on the caudal aspect of the humeral condyle at 92% of humeral length (line 4). Overall humeral torsion is the angle between lines 1 and 4; humeral torsion is –17.4°, 1.4°, and 18.1° for panels A, B, and C, respectively. For panels D through F, version of the humeral head is the angle between the humeral head datum plane (line 5) and the epicondyle datum plane (line 6). Humeral head version is –59.4°, –75.9°, and –94.8° for panels D, E, and F, respectively. For panels G through I, version of the greater tubercle is the angle between the greater tubercle datum plane (line 7) and epicondyle datum plane (line 8). Version of the greater tubercle is –178.4°, –85.9°, and 177.3° for panels, G, H, and I, respectively.

HA, mCaPHA, mCrDHA, and craniocaudal CFI were calculated.

Measurements of cortical thickness, humeral head radius of curvature, humeral head offset, greater tubercle offset, and glenoid cavity radius of curvature were indexed by dividing the values by body weight$^{0.33}$ to control for size.[17] Body weight; humeral length; torsion at the proximal, diaphyseal, and distal portions of the humerus; cortical thickness on the cranial, caudal, lateral, and medial aspects of the shaft at 20%, 30%, 40%, and 50% of humeral length; radius, version, and offset of the humeral head; version and offset of the greater tubercle; radius of the glenoid cavity; glenohumeral conformity index (calculated as radius of curvature of the humeral head/radius of curvature of the glenoid cavity)[18]; mLDHA; mCaPHA; mCrDHA[13]; shaft curvature at the proximal metaphysis of the humerus; shaft curvature at the proximal portion of the diaphysis of the humerus; and shaft curvature at the proximal portion of the humerus were compared among dogs with low, medium, and high CFI by use of an ANOVA. A Bonferroni correction was used to adjust for multiple testing; values were considered significant in the ANOVA at $P < 0.0009$. For values that differed significantly in the ANOVA, mean differences were compared for significance at a value of $P < 0.05$. Pearson correlations and paired *t* tests were used to compare shaft curvature angles from CT and radiographic measurements. Pearson correlations of humeral angulation, humeral torsion, craniocaudal CFI, and mediolateral CFI with age, body weight, and humeral length were calculated. The Pearson correlation between craniocaudal CFI and mediolateral CFI was calculated. Analyses were performed by use of statistical analysis software.[b]

Results

A randomization function[a] was used to select 40 of the 92 eligible CT examinations for analysis. There were 27 male dogs and 13 female dogs. Mean ± SD age was 3.9 ± 2.7 years, and mean body weight was 35.9 ± 10.7 kg **(Table 1)**. Thirty-five humeri were from purebred dogs, and 5 were from mixed-breed dogs. There were 13, 14, and 13 dogs in the low, medium, and high craniocaudal CFI groups, respectively. Thirteen Labrador Retrievers were included (4, 4, and 5 in the low, medium, and high craniocaudal CFI groups, respectively). There were 3 Golden Retrievers (1 in the low craniocaudal CFI group and 2 in the medium craniocaudal CFI group). There were 2 German Shepherd Dogs (1 in the low craniocaudal CFI group and 1 in the medium craniocaudal CFI group).

Mean humeral head inclination was 129°, humeral head version was -76° (the humeral head was caudal and slightly medial to the anatomic axis), and humeral head offset was 19 mm. Humeral head radius of curvature, glenoid cavity curvature, and glenohumeral conformity index were consistent among dogs

Table 1—Mean ± SD values for age, body weight, and 3-D geometric humeral measurements for 40 skeletally mature nonchondrodystrophic dogs.

Variable	Low CFI (n = 13)	Medium CFI (n = 14)	High CFI (n = 13)	Overall (n = 40)	95% CI	Absolute CV (%)
Age (y)	4.5 ± 3.1	3.6 ± 2.5	3.5 ± 2.7	3.9 ± 2.7	NA	71
Body weight (kg)	40.4 ± 13.0	36.2 ± 10.4	31.2 ± 6.5	35.9 ± 10.7	NA	30
Humeral length (mm)	196.6 ± 21.5	190.6 ± 16.5	179.1 ± 15.6	188.8 ± 19.0	182.9 to 194.7	10
Torsion (°)*						
Proximal	36.6 ± 4.6	35.7 ± 5.5	31.2 ± 8.0	34.5 ± 6.5	32.5 to 36.5	19
Metaphyseal	6.4 ± 6.9	12.6 ± 6.9	6.8 ± 6.7	8.7 ± 7.3	6.4 to 11.0	84
Distal	–46.4 ± 7.4	–45.6 ± 12.4	–42.0 ± 4.3	–44.7 ± 8.8	–47.4 to –42.0	20
Overall	–3.4 ± 5.2	2.7 ± 9.2	–4.0 ± 7.2	–1.5 ± 7.9	–3.9 to 1.0	532
Craniocaudal canal width (mm)						
20% of humeral length	27.4 ± 4.9	26.2 ± 4.0	24.7 ± 5.6	26.1 ± 4.8	24.6 to 27.6	19
50% of humeral length	17.8 ± 3.3	15.1 ± 2.3	12.7 ± 2.8	15.2 ± 3.5	14.1 to 16.3	23
Craniocaudal CFI	1.54 ± 0.09	1.73 ± 0.06	1.94 ± 0.07	1.74 ± 0.18	1.68 to 1.79	10
Mediolateral canal width (mm)						
20% of humeral length	15.1 ± 2.6	14.3 ± 2.6	12.3 ± 1.8	13.9 ± 2.6	13.1 to 14.7	19
50% of humeral length	12.0 ± 2.3	10.5 ± 2.3	8.9 ± 1.9	10.5 ± 2.5	9.7 to 11.2	23
Mediolateral CFI	1.27 ± 0.12	1.37 ± 0.11	1.40 ± 0.15	1.35 ± 0.14	1.30 to 1.39	10
Humeral head						
Radius of curvature (mm)	14.4 ± 1.7	13.6 ± 1.9	13.1 ± 1.8	13.7 ± 1.8	13.12 to 14.26	13
Indexed radius of curvature (mm/kg$^{0.33}$)†	1.13 ± 0.23	1.17 ± 0.21	1.30 ± 0.24	1.20 ± 0.23	1.13 to 1.27	19
Inclination (°)	130.4 ± 5.2	127.7 ± 8.1	128.7 ± 11.1	128.9 ± 8.4	126.3 to 131.5	6
Version (°)	–76.5 ± 9.3	–77.6 ± 11.4	–73.4 ± 7.9	–75.9 ± 9.6	–78.9 to –72.9	13
Offset (mm)	20.4 ± 4.2	19.4 ± 3.1	18.4 ± 3.4	19.4 ± 3.6	18.3 to 20.5	18
Indexed offset (mm/kg$^{0.33}$)†	1.60 ± 0.39	1.69 ± 0.39	1.80 ± 0.30	1.70 ± 0.37	1.59 to 1.81	21
Greater tubercle						
Inclination (°)	170.6 ± 3.7	170.2 ± 6.0	170.3 ± 3.9	170.4 ± 4.6	169.0 to 171.8	3
Version (°)	–54.1 ± 147.0	–43.3 ± 153.2	–21.6 ± 154.7	–39.8 ± 148.4	–85.7 to 6.2	373
Offset (mm)	6.5 ± 2.8	5.9 ± 3.0	5.4 ± 2.3	5.9 ± 2.7	5.1 to 6.8	45
Indexed offset (mm/kg$^{0.33}$)†	0.49 ± 0.14	0.50 ± 0.20	0.55 ± 0.27	0.51 ± 0.20	0.45 to 0.57	40
Shaft curvature (°)						
20% to 40% of humeral length	12.8 ± 3.8	11.6 ± 2.1	12.2 ± 4.3	12.2 ± 3.5	11.1 to 13.2	28
30% to 50% of humeral length	8.0 ± 2.1	8.5 ± 2.0	8.2 ± 2.5	8.2 ± 2.2	7.6 to 8.9	26
20% to 50% of humeral length	20.8 ± 4.6	20.1 ± 2.3	20.4 ± 5.9	20.4 ± 4.4	19.0 to 21.8	21
mCaPHA (°)	49.0 ± 3.9	50.3 ± 3.5	51.2 ± 5.9	50.2 ± 4.5	48.8 to 51.6	9
mCrDHA (°)	73.9 ± 9.5	71.5 ± 5.5	73.2 ± 8.5	72.9 ± 7.8	70.4 to 75.3	11
mLDHA (°)	88.7 ± 3.8	88.7 ± 4.2	90.4 ± 3.5	90.0 ± 3.6	88.3 to 90.6	4
Glenoid cavity						
Radius of curvature (mm)	19.5 ± 2.2	18.0 ± 1.7	17.6 ± 2.8	18.4 ± 2.3	17.6 to 19.1	13
Indexed radius of curvature (mm/kg$^{0.33}$)†	1.55 ± 0.36	1.57 ± 0.31	1.73 ± 0.25	1.61 ± 0.31	1.52 to 1.71	19
Glenohumeral conformity index	0.73 ± 0.05	0.75 ± 0.07	0.75 ± 0.07	0.75 ± 0.06	0.73 to 0.76	8

The CFI was classified as follows: high (CFI > 1.83), medium (1.64 ≤ CFI ≤ 1.83), and low (CFI < 1.64).

*For torsion, proximal represents the proximal portion of the humerus (8% to 20% of humeral length), diaphyseal represents the diaphyseal portion of the humerus (20% to 75% of humeral length), distal represents the distal portion of the humerus (75% to 92% of humeral length), and overall represents 8% to 92% of humeral length.

†Values were indexed on the basis of body weight$^{0.33}$.

CI = Confidence interval. CV = Coefficient of variation. NA = Not applicable.

(all had coefficients of variation < 14%). Mean inclination of the greater tubercle was 170°, greater tubercle version was −40°, and greater tubercle offset was 6 mm. The proximal aspect of the greater tubercle was always lateral to the anatomic axis but was caudal (26/40 [65%] dogs) or cranial (14/40 [35%] dogs) to that axis. Mean shaft curvature was 20°. Shaft curvature from 20% to 40% of humeral length was significantly ($P < 0.0001$; ANOVA followed by Bonferroni correction) greater (3.9 ± 3.8° greater) than the shaft curvature from 30% to 50% of humeral length. Curvatures at 20% to 40% of humeral length and at 30% to 50% of humeral length did not have a significant linear relationship ($r = 0.16$; $P = 0.320$). Humeral shaft angulation was not significantly correlated with body weight ($r = 0.14$; $P = 0.419$), humeral length ($r = -0.05$; $P = 0.778$), or age ($r = -0.20$; $P = 0.237$).

Craniocaudal CFI for Labrador Retrievers ranged from 1.37 to 2.10 **(Figure 3)**. One Labrador Retriever had the lowest CFI, and another Labrador Retriever had the highest CFI, among dogs included in the study. Craniocaudal CFI was significantly correlated with body weight ($r = -0.34$; $P = 0.031$) and humeral length ($r = -0.40$; $P = 0.012$). Craniocaudal CFI and age were not significantly correlated for males ($r = -0.17$; $P = 0.384$), females ($r = -0.32$; $P = 0.279$), or males and females combined ($r = -0.23$; $P = 0.160$). Mediolateral CFI was significantly correlated with humeral length ($r = -0.33$; $P = 0.040$) but not with body weight ($r = -0.25$; $P = 0.138$) or age ($r = -0.08$;

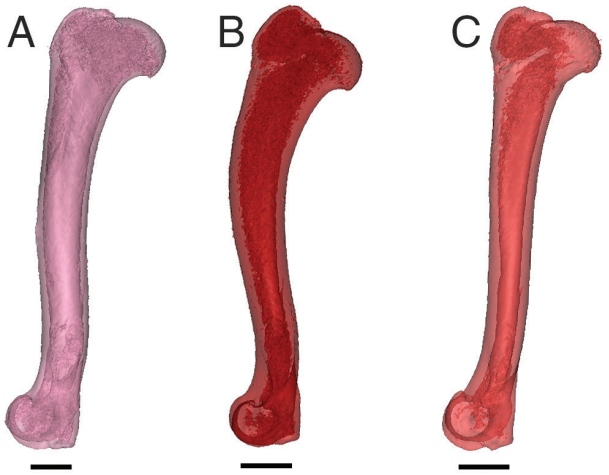

Figure 3—Semitransparent 3-D drawings of a humerus from a 10-year-old Alaskan Malamute (A), 1-year-old Labrador Retriever (B), and 1-year-old Siberian Husky (C). The Alaskan Malamute had a stovepipe humerus with a low craniocaudal CFI of 1.39 and curvature of the shaft from 20% to 50% of humeral length of 11.6°. The Labrador Retriever had a humerus with a medium craniocaudal CFI of 1.73 and curvature of the shaft from 20% to 50% of humeral length of 26.4°. The Siberian Husky had a champagne-fluted humerus with a high craniocaudal CFI of 2.02 and curvature of the shaft from 20% to 50% of humeral length of 9.6°. Notice that the magnification differs among bones. Bar = 20 mm.

P = 0.637). Craniocaudal and mediolateral CFI were significantly correlated (*r* = 0.38; *P* = 0.018). Humeral torsion was not significantly correlated with body weight (*r* = 0.23; *P* = 0.168), humeral length (*r* = 0.13; *P* = 0.439), or age (*r* = 0.22; *P* = 0.194).

Cranial cortical thickness at 30% of humeral length was significantly greater for dogs with high craniocaudal CFI than low craniocaudal CFI (*P* = 0.0007; ANOVA followed by Bonferroni correction) but not medium craniocaudal CFI (*P* = 0.007; ANOVA followed by Bonferroni correction) and did not differ significantly (*P* = 0.641) between dogs with medium and low craniocaudal CFI **(Table 2)**. Medial cortical thickness at 30% of humeral length was significantly greater for dogs with high craniocaudal CFI than low craniocaudal CFI (*P* = 0.0004; ANOVA followed by Bonferroni correction) but not medium craniocaudal CFI (*P* = 0.025; ANOVA followed by Bonferroni correction) and did not differ significantly (*P* = 0.277) between dogs with medium and low craniocaudal CFI. Cranial cortical thickness at 40% of humeral length was significantly greater for dogs with high craniocaudal CFI than low craniocaudal CFI (*P* < 0.0001; ANOVA followed by Bonferroni correction) but not medium craniocaudal CFI (*P* = 0.001; ANOVA followed by Bonferroni correction) and did not differ significantly (*P* = 0.545) between dogs with medium and low craniocaudal CFI. Medial cortical thickness at 40% of humeral length was significantly greater in dogs with high craniocaudal CFI than low craniocaudal CFI (*P* = 0.0005; ANOVA followed by Bonferroni correction) but did not differ between dogs with high and medium craniocaudal CFI (*P* = 0.115) or medium and low CFI (*P* = 0.058). Medial cortical thickness at 50% of humeral length was significantly greater in dogs with high craniocaudal CFI than low craniocaudal CFI (*P* = 0.0005; ANOVA followed by Bonferroni correction) but not medium craniocaudal CFI (*P* = 0.039; ANOVA followed by Bonferroni correction) and did not differ significantly (*P* = 0.212) between dogs with medium and low craniocaudal CFI. Body weight; humeral length; radius of curvature of the glenoid cavity; radius of curvature, version, and offset of the humeral head; glenohumeral conformity; version and offset of the greater tubercle; humeral torsion (proximal, diaphyseal, and distal portions of the humerus); humeral shaft angulation (proximal metaphysis, proximal portion of the diaphysis, and overall); mLDHA; mCaPHA; and mCrDHA did not differ significantly (*P* ranged from 0.0386 to 0.9225; ANOVA followed by Bonferroni correction) among groups with various CFIs. Cranial, caudal, lateral, and medial cortical thickness at 20% of humeral length; caudal and lateral cortical thickness at 30% of humeral length; caudal and lateral cortical thickness at 40% of humeral length; and cranial, caudal, and lateral cortical thickness at 50% of humeral length did not differ significantly (*P* ranged from 0.0017 to 0.0783; ANOVA followed by Bonferroni correction) among groups with various CFIs.

The 38 dogs that were used for radiographic measurements had a mean ± SD body weight of 32.3 ± 8.7 kg and were 8.5 ± 3.7 years old. Mean radiographic craniocaudal CFI index was 1.99 ± 0.22, mean shaft curvature from 20% to 40% of humeral length was 7.8 ± 4.2°, mean shaft curvature from 30% to 50% of humeral length was 8.0 ± 4.5°, mean shaft curvature from 20% to 50% of humeral length was 15.8 ± 5.6°, mean mCaPHA was 49.3 ± 4.9°, mean mCrDHA was 70.0 ± 5.6°, and mean mLDHA was 90.2 ± 3.7°. Craniocaudal CFI measured on radiographs was significantly (*P* < 0.0001; ANOVA followed by Bonferroni correction) greater (0.25 greater) than the craniocaudal CFI measured on CT images. Shaft curvature from 20% to 40% of humeral length was significantly (*P* < 0.0001; ANOVA followed by Bonferroni correction) less (4.4° less) for radiographic measurements than for CT measurements. Shaft curvature from 30% to 50% of humeral length was less (0.2° less) for radiographic measurements than for CT measurements, but these values did not differ significantly (*P* = 0.805). Shaft curvature from 20% to 50% of humeral length was significantly (*P* < 0.0001; ANOVA followed by Bonferroni correction) less (4.6° less) for radiographic measurements than for CT measurements. The 95% confidence intervals for shaft curvature for radiographic and CT measurements were 14° to 17.6° and 19.0° to 21.8°, respectively. Radiographic and CT measurements of mLDHA, mCaPHA, and mCrDHA did not differ significantly (*P* = 0.368, 0.429, and 0.066, respectively).

Table 2—Mean ± SD values for cortical thickness and indexed* cortical thickness of the humerus of 40 skeletally mature nonchondrodystrophic dogs grouped on the basis of craniocaudal CFI.

Variable	Low CFI (n = 13)	Medium CFI (n = 14)	High CFI (n = 13)	Overall (n = 40)
20% of humeral length				
Cranial aspect (mm)	1.7 ± 0.5	1.7 ± 1.1	1.8 ± 0.4	1.7 ± 0.7
Cranial aspect, indexed (mm/kg$^{0.33}$)	0.14 ± 0.06	0.14 ± 0.04	0.19 ± 0.07	0.15 ± 0.06
Caudal aspect (mm)	1.4 ± 0.4	2.1 ± 0.9	2.1 ± 0.7	1.9 ± 0.8
Caudal aspect, indexed (mm/kg$^{0.33}$)	0.11 ± 0.03	0.18 ± 0.08	0.20 ± 0.05	0.16 ± 0.07
Lateral aspect (mm)	1.8 ± 0.5	1.8 ± 0.3	2.1 ± 0.5	1.9 ± 0.4
Lateral aspect, indexed (mm/kg$^{0.33}$)	0.15 ± 0.06	0.16 ± 0.05	0.21 ± 0.06	0.17 ± 0.06
Medial aspect (mm)	2.1 ± 0.6	1.9 ± 0.5	2.1 ± 0.4	2.0 ± 0.5
Medial aspect, indexed (mm/kg$^{0.33}$)	0.16 ± 0.03	0.16 ± 0.04	0.21 ± 0.05	0.18 ± 0.05
30% of humeral length				
Cranial aspect (mm)	2.2 ± 0.7	2.3 ± 0.6	2.9 ± 0.7	2.5 ± 0.7
Cranial aspect, indexed (mm/kg$^{0.33}$)	0.18 ± 0.05^{a}	0.20 ± 0.06^{ab}	0.29 ± 0.10^{b}	0.22 ± 0.09
Caudal aspect (mm)	2.3 ± 0.6	2.7 ± 0.8	2.8 ± 0.7	2.6 ± 0.7
Caudal aspect, indexed (mm/kg$^{0.33}$)	0.18 ± 0.04	0.24 ± 0.08	0.27 ± 0.06	0.23 ± 0.07
Lateral aspect (mm)	2.0 ± 0.4	2.4 ± 0.6	2.4 ± 0.5	2.3 ± 0.6
Lateral aspect, indexed (mm/kg$^{0.33}$)	0.17 ± 0.06	0.21 ± 0.08	0.24 ± 0.07	0.21 ± 0.07
Medial aspect (mm)	2.1 ± 0.6	2.2 ± 0.5	2.5 ± 0.5	2.3 ± 0.6
Medial aspect, indexed (mm/kg$^{0.33}$)	0.16 ± 0.04^{a}	0.19 ± 0.07^{ab}	0.25 ± 0.05^{b}	0.20 ± 0.06
40% of humeral length				
Cranial aspect (mm)	2.8 ± 0.6	2.9 ± 0.9	3.5 ± 0.9	3.1 ± 0.9
Cranial aspect, indexed (mm/kg$^{0.33}$)	0.22 ± 0.06^{a}	0.25 ± 0.05^{ab}	0.35 ± 0.09^{b}	0.27 ± 0.09
Caudal aspect (mm)	3.2 ± 0.7	2.9 ± 0.6	3.2 ± 0.7	3.1 ± 0.7
Caudal aspect, indexed (mm/kg$^{0.33}$)	0.25 ± 0.06	0.26 ± 0.08	0.31 ± 0.06	0.27 ± 0.07
Lateral aspect (mm)	2.3 ± 0.4	2.5 ± 0.5	2.5 ± 0.2	2.4 ± 0.4
Lateral aspect, indexed (mm/kg$^{0.33}$)	0.18 ± 0.05	0.22 ± 0.06	0.25 ± 0.06	0.21 ± 0.06
Medial aspect (mm)	2.1 ± 0.4	2.5 ± 0.8	2.6 ± 0.4	2.4 ± 0.6
Medial aspect, indexed (mm/kg$^{0.33}$)	0.16 ± 0.04^{a}	0.21 ± 0.06^{ab}	0.26 ± 0.06^{b}	0.21 ± 0.07
50% of humeral length				
Cranial aspect (mm)	3.0 ± 0.4	3.2 ± 1.1	3.4 ± 0.5	3.2 ± 0.7
Cranial aspect, indexed (mm/kg$^{0.33}$)	0.24 ± 0.07	0.27 ± 0.08	0.34 ± 0.09	0.28 ± 0.09
Caudal aspect (mm)	3.2 ± 0.6	3.1 ± 0.5	3.3 ± 0.6	3.2 ± 0.6
Caudal aspect, indexed (mm/kg$^{0.33}$)	0.25 ± 0.07	0.27 ± 0.06	0.32 ± 0.07	0.28 ± 0.07
Lateral aspect (mm)	2.7 ± 0.5	2.7 ± 0.5	2.8 ± 0.3	2.7 ± 0.4
Lateral aspect, indexed (mm/kg$^{0.33}$)	0.21 ± 0.05	0.24 ± 0.06	0.28 ± 0.06	0.24 ± 0.06
Medial aspect (mm)	2.5 ± 0.4	2.7 ± 0.5	3.0 ± 0.4	2.7 ± 0.5
Medial aspect, indexed (mm/kg$^{0.33}$)	0.20 ± 0.06^{a}	0.23 ± 0.06^{ab}	0.29 ± 0.06^{b}	0.24 ± 0.07

*Values were indexed on the basis of body weight$^{0.33}$.

^{a,b}Within a row, values with different superscript letters differ significantly ($P < 0.05$).

Discussion

In the present study, the 3-D geometry of the canine humerus was evaluated for a group of skeletally mature nonchondrodystrophic dogs with the intent of gathering information for use in the design of a prosthetic stem. Although stemless total shoulder joint arthroplasty is emerging for use in humans and has been used in 1 dog,[19,20] most shoulder joint arthroplasties involve the use of a stem introduced in the humeral medullary canal. Because a more anatomic reconstruction of the shoulder joint after total shoulder joint replacement in humans is associated with improved outcomes,[21–23] it was logical to gather information about the geometric variability of the canine humerus before designing a prosthetic stem. Humeral geometries of dogs with differing humeral CFI were compared to determine whether specific geometric patterns were associated with low or high CFI (as has been suggested for the femur, whereby large femurs have a low CFI and thin cortices[24,c]). The CT measurements were compared with radiographic measurements collected from another group of dogs to evaluate whether radiographic and CT assessments of humeral geometry would be interchangeable.

Position (inclination, version, and offset) of the humeral head in relation to the anatomic axis was consistent among dogs and was not influenced by CFI. Humeral head retroversion was 76°, which indicated that the humeral head was predominantly caudal and slightly medial to the mechanical axis of the femur. Version was variable, with a range of approximately 40°. By comparison, mean humeral retroversion in humans ranges from 13° to 21°.[1,7,18,25–27] Retroversion of the humeral head in humans is also variable, with a range of approximately 55°.[7,28] For the canine femur, mean anteversion was 20° and 30°, with a range of approximately 20°, for studies[29,30] that involved the use of CT reconstructions. Mean humeral head inclination was 130° in the present study. By comparison, mean humeral head inclination in humans ranges from 130° to 141°.[1,7,18,25] Prosthetic stem inclination for total shoulder joint implants of humans generally ranges from 125° to 155°.[31–33] Inclination of humeral prosthetic stems for humans can be fixed,[34,35] modu-

lar through the use of a range of humeral heads,[31] or fully adjustable during surgery.[28,33,35,f] Mean femoral head inclination of dogs was 128° in a study[30] that involved the use of CT reconstruction. For commercially available total hip joint stems, inclination is 135° for 2 stems from one manufacturer[g,h] and 145° for 1 stem from another manufacturer.[i] The influence of prosthetic geometry on prosthetic range of motion and impingement has been discussed extensively for replacement of hip and shoulder joints of humans[36,37] and is an emerging topic for hip joint replacement in dogs.[38] Mean humeral head offset in the present study was 19 mm. By comparison, mean humeral head offset in humans ranges from 6 to 10 mm.[7,18,25,39] Prosthetic humeral head offset generally is 3 to 4 mm.[28,35] Mean femoral head offset was 16 mm for mixed-breed dogs of one study[40] and 20 mm for Greyhounds of another study.[41] Prosthetic femoral head offset ranges from 11.3 to 34.3 mm for cemented prosthetic hip stems[g] and from 12.7 to 30.1 mm for cementless prosthetic hip joint stems[h] from one manufacturer and from 14.6 to 20.4 mm for cementless prosthetic hip joint stems from another manufacturer,[i] as determined on the basis of stem and head size.

For the greater tubercle in the present study, mean inclination was 170°, mean retroversion was 40°, and mean offset was 6 mm. The range for greater tubercle version was wide (90°) because although the greater tubercle was lateral to the anatomic axis in all dogs, it was caudal to the axis in two-thirds of the dogs and cranial to the axis in one-third of the dogs. That variability relative to the anatomic axis most likely resulted from differences in the shape of the greater tubercle (whereby the proximal aspect of the greater tubercle can be more or less cranial on the trochanter) and from differences in shaft curvature. Curvature range was approximately 20°. Increased curvature for the proximal metaphysis increased the likelihood that the greater tubercle would be caudal to the anatomic axis. Canal flare index did not influence the position of the greater tubercle. The shape and position of long-bone apophyses relative to anatomic axes of those long bones has rarely been assessed by use of 3-D modeling for dogs or humans. In 1 report[42] of 7 humans, anteversion of the greater trochanter also ranged widely (from 17° to 73°). The wide range in version of apophyses suggests that further research is warranted to characterize the shape and position of long-bone apophyses because their position may interfere with the insertion of prosthetic components (ie, greater trochanter) and could be linked with pathological changes of tendons (ie, supraspinatus insertionopathy or iliopsoas tendinopathy).

The radii of curvature for the humeral head and glenoid cavity were consistent among dogs and relative to each other (radius of curvature for the humeral head was approximately 75% of the radius of curvature for the glenoid cavity). By comparison, that ratio in humans is 56%[43] or 63%.[18] In humans, shoulder joint luxation has been associated with increases in the craniocaudal and mediolateral radius of curvature of the humeral head.[43] It is unclear whether shoulder joint diseases in dogs are associated with abnormal curvature of the humeral head or glenoid cavity. A potential decrease in the glenoid cavity curvature in a dog with osteochondritis dissecans of the glenoid cavity has been reported.[44]

Mean craniocaudal curvature of the humeral shaft was approximately 20° in the present study. That curvature was not uniform because curvature of the proximal metaphysis (approx 12°) was approximately 1.5 times as great as the curvature of the proximal portion of the diaphysis (8°). Therefore, we rejected the hypothesis that curvature of the proximal portion of the humeral shaft was uniform. Nonuniform curvature complicates insertion of a curved prosthetic stem because curved broaches and stems need to follow a uniformly curved track to maintain contact with endosteal surfaces.[45] The study reported here evaluated curvature of the proximal half of the humerus because the focus of the study was total shoulder joint replacement. There is also curvature in the distal metaphysis of the humerus. Subjectively, curvature of the distal portion of the humerus is less than the curvature of the proximal portion of the humerus. The humeral shaft of humans has anterior curvature. In 1 report,[46] anterior curvature of the shaft of humans was 9 ± 3° and originated in the distal metaphysis. In humans, femoral curvature is associated with bone size because longer femurs have less curvature than do shorter femurs.[47] A similar association was not identified in the present study. Maximal curvature of the canine femur originates in the distal metaphysis and is located caudally.[41,48] Mean overall torsion of the humeral shaft in the present study was small (1.5° of internal torsion), with a range of 37°. There was a similar range of 36° for humeral torsions of humans in 1 study.[26]

Mean craniocaudal CFI (1.74) for dogs of the present study was less than that for the humerus of humans (2.8).[18] Craniocaudal CFI was lower in heavier dogs and for longer humeri. The coefficient of variation was 10% for both mediolateral and craniocaudal CFI. By comparison, the coefficient of variation for mediolateral CFI in the canine femur was 5% (11 femurs with a fracture) and 2% (73 femurs without a fracture) in dogs undergoing total hip joint replacement[24] and was 13% in a study[49] that included 24 dogs of various breeds.This suggests that canal flare is likely similar in the canine humerus and femur. An association between shaft curvature and CFI was not identified in the present study. Therefore, we rejected the hypothesis that a large CFI was associated with large values for shaft curvature.

In the present study, humeral CFI was not influenced by age. Femoral canal flare in humans decreases as age increases.[50,51] However, femoral canal CFI was not influenced by age for 42 Greyhounds[41] and for 26 dogs of various breeds.[e] Femoral canal flare in-

fluences the stability of cementless stems and the risk of fracture after cementless hip joint replacement in dogs. In 1 in vitro study,[15] stems implanted in femurs with a low CFI were 6 times as likely to subside (ie, migrate down the femoral shaft) under load as stems implanted in femurs with a normal CFI and 72 times as likely to subside as stems implanted in femurs with a high CFI. In another study[24] of cementless total hip joint replacement, dogs with postoperative femoral fractures had a mean mediolateral CFI of 1.80, compared with 1.98 for dogs without fractures.

Radiographic and CT measurements of angles that defined the mediolateral and craniocaudal orientation of epiphyses relative to the diaphysis did not differ. However, radiographic measurements of craniocaudal curvature were less than CT measurements. Therefore, we rejected the hypothesis that CT and radiographic measurements of humeral shaft angulation did not differ. That difference in angulation could have been attributable to the fact that bones were precisely oriented for CT measurement but radiographs were potentially acquired while the humerus was internally or externally rotated from a true mediolateral view, which would decrease the apparent curvature. Alternatively, the difference could have been the result of a disparity between the dogs evaluated radiographically and by use of CT. Further assessment of the relationship between radiographic and 3-D measurements of curvature will require comparison of radiographs and CT images obtained from the same dogs and will be helpful for assessing the accuracy of radiographs for use in surgical planning. In the present study, radiographic craniocaudal CFI measurements were 13% less than CFI measurements for CT images. Similarly, radiographic mediolateral CFI measurements obtained for radiographs of 300 human femurs were 12% less than mediolateral CFI measurements obtained for CT images of the same femurs (3.81 ± 0.83 vs 4.32 ± 1.05, respectively).[5]

The 3-D geometry of the humerus of dogs was evaluated in the study reported here. Humeri had a nonuniform curvature that was greater in the proximal metaphysis than in the proximal portion of the diaphysis. Humeral head retroversion was comparable to femoral head anteversion, humeral head inclination was comparable to femoral head inclination, and craniocaudal humeral CFI was comparable to mediolateral femoral CFI, which suggested that a prosthetic stem for total shoulder joint replacement could have a shape comparable to that of prosthetic stems for total hip joint replacement. Radiographic and CT measurements of CFI and curvature did not appear to be interchangeable.

Acknowledgments

This manuscript represents a portion of a thesis submitted by Ms. Smith to the Joint North Carolina State University–University of North Carolina at Chapel Hill Department of Biomedical Engineering as partial fulfillment of the requirements for a Master of Science degree.

Information reported in this manuscript was based on research supported by a Dissertation Completion Fellowship from the graduate school at the University of North Carolina at Chapel Hill.

The authors thank Melanie Card for technical assistance.

Footnotes

a. Excel for Mac 2011, version 14.4.8, Microsoft Corp, Redmond, Wash.
b. SAS, version 9.4, SAS Institute Inc, Cary, NC.
c. Mimics Innovation Suite, version 18.0, Materialise, Plymouth, Mich.
d. 3-matic, version 10.0, Materialise, Plymouth, Mich.
e. Pugliese LC. Proximal femoral morphology and bone quality assessment in dogs. MS thesis, Department of Veterinary Clinical Science, College of Veterinary Medicine, The Ohio State University, Columbus, Ohio, 2014.
f. Anatomic shoulder system, Zimmer, Warsaw, Ind. Available at: www.zimmer.com/content/dam/zimmer-web/documents/en-US/pdf/medical-professionals/shoulder/Anatomical-Shoulder-System-Brochure-06.009.920.12-Rev-4-09-2010.pdf. Accessed Nov 9, 2016.
g. CFX femoral stem, BioMedtrix, Whippany, NJ.
h. BFX femoral stem, BioMedtrix, Whippany, NJ.
i. Zurich stem, Kyon Veterinary Surgical Products, Boston, Mass.

References

1. Robertson DD, Yuan J, Bigliani LU, et al. Three-dimensional analysis of the proximal part of the humerus: relevance to arthroplasty. *J Bone Joint Surg Am* 2000;82-A:1594–1602.
2. Desai SJ, Deluce S, Johnson JA, et al. An anthropometric study of the distal humerus. *J Shoulder Elbow Surg* 2014;23:463–469.
3. Faizan A, Wuestemann T, Nevelos J, et al. Development and verification of a cementless novel tapered wedge stem for total hip arthroplasty. *J Arthroplasty* 2015;30:235–240.
4. Alolabi B, Studer A, Gray A, et al. Selecting the diameter of a radial head implant: an assessment of local landmarks. *J Shoulder Elbow Surg* 2013;22:1395–1399.
5. Husmann O, Rubin PJ, Leyvraz PF, et al. Three-dimensional morphology of the proximal femur. *J Arthroplasty* 1997;12:444–450.
6. Schumann S, Tannast M, Nolte LP, et al. Validation of statistical shape model based reconstruction of the proximal femur—a morphology study. *Med Eng Phys* 2010;32:638–644.
7. Boileau P, Walch G. The three-dimensional geometry of the proximal humerus. Implications for surgical technique and prosthetic design. *J Bone Joint Surg Br* 1997;79:857–865.
8. Bouza-Rodríguez JB, Miramontes-Sequeiros LC. Three-dimensional biomechanical analysis of the bovine humerus. *Appl Bionics Biomech* 2014;11:13–24.
9. Maddox TW, May C, Keeley BJ, et al. Comparison between shoulder computed tomography and clinical findings in 89 dogs presented for thoracic limb lameness. *Vet Radiol Ultrasound* 2013;54:358–364.
10. Kalff S, Gemmill T. Proximal focal humeral deficiency in a large breed dog. *Vet Comp Orthop Traumatol* 2012;25:532–536.
11. Morgan JP, Pool RR, Miyabayashi T. Primary degenerative joint disease of the shoulder in a colony of Beagles. *J Am Vet Med Assoc* 1987;190:531–540.
12. Fitzpatrick N, Yeadon R, Smith TJ, et al. Shoulder arthrodesis in 14 dogs (Erratum published in *Vet Surg* 2013;42:229). *Vet Surg* 2012;41:745–754.
13. Wood MC, Fox DB, Tomlinson JL. Determination of the mechanical axis and joint orientation lines in the canine humerus: a radiographic cadaveric study. *Vet Surg* 2014;43:414–417.
14. Smith EJ, Marcellin-Little DJ, Harrysson OL, et al. Influence of chondrodystrophy and brachycephaly on geometry of the humerus in dogs. *Vet Comp Orthop Traumatol* 2016;29:220–226.
15. Rashmir-Raven AM, DeYoung DJ, Abrams CF Jr, et al. Subsidence of an uncemented canine femoral stem. *Vet Surg* 1992;21:327–331.
16. Kwan TW, Marcellin-Little DJ, Harrysson OL. Correction of biapical radial deformities by use of bi-level hinged circular external fixation and distraction osteogenesis in 13 dogs. *Vet Surg* 2014;43:316–329.

17. Sisson D, Schaeffer D. Changes in linear dimensions of the heart, relative to body weight, as measured by M-mode echocardiography in growing dogs. *Am J Vet Res* 1991;52:1591–1596.
18. McPherson EJ, Friedman RJ, An YH, et al. Anthropometric study of normal glenohumeral relationships. *J Shoulder Elbow Surg* 1997;6:105–112.
19. Churchill RS. Stemless shoulder arthroplasty: current status. *J Shoulder Elbow Surg* 2014;23:1409–1414.
20. Sparrow T, Fitzpatrick N, Meswania J, et al. Shoulder joint hemiarthroplasty for treatment of a severe osteochondritis dissecans lesion in a dog. *Vet Comp Orthop Traumatol* 2014;27:243–248.
21. Flurin PH, Roche CP, Wright TW, et al. Correlation between clinical outcomes and anatomic reconstruction with anatomic total shoulder arthroplasty. *Bull Hosp Jt Dis* 2015;73:S92–S98.
22. Kadum B, Wahlstrom P, Khoschnau S, et al. Association of lateral humeral offset with functional outcome and geometric restoration in stemless total shoulder arthroplasty. *J Shoulder Elbow Surg* 2016;25:e285–e294.
23. Renkawitz T, Weber T, Dullien S, et al. Leg length and offset differences above 5 mm after total hip arthroplasty are associated with altered gait kinematics. *Gait Posture* 2016;49:196–201.
24. Ganz SM, Jackson J, VanEnkevort B. Risk factors for femoral fracture after canine press-fit cementless total hip arthroplasty. *Vet Surg* 2010;39:688–695.
25. Hertel R, Knothe U, Ballmer FT. Geometry of the proximal humerus and implications for prosthetic design. *J Shoulder Elbow Surg* 2002;11:331–338.
26. Krahl VE, Evans FG. Humeral torsion in man. *Am J Phys Anthropol* 1945;3:229–253.
27. Roberts SN, Foley AP, Swallow HM, et al. The geometry of the humeral head and the design of prostheses. *J Bone Joint Surg Br* 1991;73:647–650.
28. Pearl ML. Proximal humeral anatomy in shoulder arthroplasty: implications for prosthetic design and surgical technique. *J Shoulder Elbow Surg* 2005;14:99S–104S.
29. Ginja MM, Gonzalo-Orden JM, Jesus SS, et al. Measurement of the femoral neck anteversion angle in the dog using computed tomography. *Vet J* 2007;174:378–383.
30. Yasukawa S, Edamura K, Tanegashima K, et al. Evaluation of bone deformities of the femur, tibia, and patella in Toy Poodles with medial patellar luxation using computed tomography. *Vet Comp Orthop Traumatol* 2016;29:29–38.
31. Walch G, Boileau P. Prosthetic adaptability: a new concept for shoulder arthroplasty. *J Shoulder Elbow Surg* 1999;8:443–451.
32. Lädermann A, Denard PJ, Boileau P, et al. Effect of humeral stem design on humeral position and range of motion in reverse shoulder arthroplasty. *Int Orthop* 2015;39:2205–2213.
33. Pearl ML, Kurutz S, Postacchini R. Geometric variables in anatomic replacement of the proximal humerus: how much prosthetic geometry is necessary? (Erratum published in *J Shoulder Elbow Surg* 2012;21:1803). *J Shoulder Elbow Surg* 2009;18:366–370.
34. Pearl ML, Kurutz S, Robertson DD, et al. Geometric analysis of selected press fit prosthetic systems for proximal humeral replacement. *J Orthop Res* 2002;20:192–197.
35. Irlenbusch U, End S, Kilic M. Differences in reconstruction of the anatomy with modern adjustable compared to second-generation shoulder prosthesis. *Int Orthop* 2011;35:705–711.
36. Malik A, Maheshwari A, Dorr LD. Impingement with total hip replacement. *J Bone Joint Surg Am* 2007;89:1832–1842.
37. Iannotti JP, Spencer EE, Winter U, et al. Prosthetic positioning in total shoulder arthroplasty. *J Shoulder Elbow Surg* 2005;14:111S–121S.
38. Roe SC, Sidebotham C, Marcellin-Little DJ. Acetabular cup liner and prosthetic head exchange to increase the head diameter for management of recurrent luxation of a prosthetic hip in two dogs. *Vet Comp Orthop Traumatol* 2015;28:60–66.
39. Pearl ML, Volk AG. Coronal plane geometry of the proximal humerus relevant to prosthetic arthroplasty. *J Shoulder Elbow Surg* 1996;5:320–326.
40. Sarierler M, Yildirim IG, Ocal MK. Effect of triple pelvic osteotomy on the proximal femoral geometry in dysplastic dogs. *Res Vet Sci* 2012;92:142–146.
41. Kuo TY, Skedros JG, Bloebaum RD. Comparison of human, primate, and canine femora: implications for biomaterials testing in total hip replacement. *J Biomed Mater Res* 1998;40:475–489.
42. Gulledge BM, Marcellin-Little DJ, Levine D, et al. Comparison of two stretching methods and optimization of stretching protocol for the piriformis muscle. *Med Eng Phys* 2014;36:212–218.
43. Peltz CD, Zauel R, Ramo N, et al. Differences in glenohumeral joint morphology between patients with anterior shoulder instability and healthy, uninjured volunteers. *J Shoulder Elbow Surg* 2015;24:1014–1020.
44. Dunlap AE, Gines JA, Simone KM, et al. What is your diagnosis? Glenoid osteochondritis dissecans in a dog. *J Am Vet Med Assoc* 2017;250:975–978.
45. Gustke K. Short stems for total hip arthroplasty: initial experience with the Fitmore stem. *J Bone Joint Surg Br* 2012;94:47–51.
46. Akpinar F, Aydinlioglu A, Tosun N, et al. A morphometric study on the humerus for intramedullary fixation. *Tohoku J Exp Med* 2003;199:35–42.
47. Su XY, Zhao Z, Zhao JX, et al. Three-dimensional analysis of the curvature of the femoral canal in 426 Chinese femurs. *Biomed Res Int* 2015;2015:318391.
48. Bloebaum RD, Ota DT, Skedros JG, et al. Comparison of human and canine external femoral morphologies in the context of total hip replacement. *J Biomed Mater Res* 1993;27:1149–1159.
49. Palierne S, Asimus E, Mathon D, et al. Geometric analysis of the proximal femur in a diverse sample of dogs. *Res Vet Sci* 2006;80:243–252.
50. Casper DS, Kim GK, Parvizi J, et al. Morphology of the proximal femur differs widely with age and sex: relevance to design and selection of femoral prostheses. *J Orthop Res* 2012;30:1162–1166.
51. Boymans TA, Heyligers IC, Grimm B. The morphology of the proximal femoral canal continues to change in the very elderly: implications for total hip arthroplasty. *J Arthroplasty* 2015;30:2328–2332.